Estimation of Enhanced Breakdown Voltages in 3C-SiC Schottky Barrier Diode using Special Erfc Distribution Doping Profiles

Dissertation submitted towards the partial fulfilment of requirement for the award of degree of

Master of Engineering

In

Electronics and Communication Engineering

Submitted by:

Priya

Roll No: 801161017

Under the guidance of:

Dr. A. K. Chatterjee

Professor, ECED

ELECTRONICS AND COMMUNICATION ENGINEERING DEPARTMENT

THAPAR UNIVERSITY

(Established under the section 3 of UGC Act, 1956)

PATIALA – 147004 (PUNJAB)

JULY 2013

CERTIFICATE

I hereby certify that the thesis entitled **"Estimation of Enhanced Breakdown Voltages in 3C-SiC Schottky Barrier Diode using Special Erfc Distribution Doping Profiles"** is an authentic record of my study carried out as requirement for the award of degree of Master of Engineering (Electronics and Communication Engineering) at Thapar University, Patiala, under the supervision of Dr. A.K.Chatterjee, Professor, Electronics and Communication Engineering Department, Thapar University, Patiala.

I have not submitted the matter presented in the thesis for the award of any other degree to any other university.

Date: 11/07/13

Priya

(801161017)

It is certified that the above statement made by the student is correct to the best of my knowledge and belief.

Date: 11/07/13

Dr. A. K. Chatterjee

Professor

ECED, Thapar University,

Patiala (Punjab)-147004

Dr. Rajesh Khanna

Professor and Head

ECED, Thapar University,

Patiala (Punjab)-147004

Dr. S.K. Mohapatra

Dean, Academic Affairs

Thapar University,

Patiala (Punjab)-147004

ACKNOWLEDGEMENT

First and foremost, I thank God for everything that has made this dissertation work possible.

I would like to sincerely thanks to my supervisor Dr. A. K. Chatterjee, Professor, Electronics & Communication Engineering Department, Thapar University, Patiala for their continuous indefatigable guidance, which paved me on to the path to carry this project. He has always been very encouraging and offered invaluable advice. I am highly indebted to them for their painstaking efforts and invaluable suggestions during the period of work.

I am also thankful to Dr. Rajesh Khanna, Professor and Head and Dr. Kulbir Singh, Associate Professor, Electronics & Communication Engineering Department, Thapar University, Patiala for their valuable advice and helped in all possible ways for the completion of my dissertation work. I wish to express thanks to all those persons who with their encouraging words and suggestions have contributed directly or indirectly for the completion of this work.

Date: -

Place: Patiala (Priya)

ABSTRACT

Normal Schottky Barrier diodes have been designed using a uniform doping of the semiconductor material used. However, the breakdown voltage obtained can be improved using non-uniform doping profiles, namely, linear graded profiles. Gaussian and Complementary error function have also been used for this purpose. However, special complementary error function for doping profiles in the semiconductor with n=1 and n=3 have been utilized in the exponential powers and it has been estimated that using peak carrier concentration $N_o = 10^{16}$ /cm^3 with complementary erfc distribution and n=3 can be utilized to design 3C-SiC Schottky Barrier diodes with breakdown voltages of 14.3 kV. These results have been represented in this work and a comparison between breakdown voltages obtained with N_o ranging from 10^{14} /cm^3 to 10^{16}/cm^3 with variation in n from 1 to 3.

Table of Contents

List of Figures

List of Tables

CHAPTER 1

Introduction

The advancement in semiconductor materials has always been one of the most significant steps towards the progression of any electronic device. Power electronic devices have considerable influence on the economy due to its extensive use in various industrial and non-industrial applications. For greater energy efficiency power devices support cost effective as well as environment friendly tools that is required for the global issues. Silicon based power electronic devices are commercially available from 1950s. They have the ability of handling significant voltage and currents and have been widely developed since then. But, the performance of these devices has been limited for high temperature as well as high power applications. However, a wide band gap semiconductor i.e. Silicon Carbide has the potential to take the place of Silicon in high power devices due to its exceptional electrical and physical properties.

1.1 Silicon vs Silicon Carbide

Silicon based high power devices have been commercially available for more than 50 years and are viewed as the vital component of almost all power electronic devices. However at high temperature environment as well as for high power applications, the performance of Si based power devices has been limited. The excellent characteristics of SiC as a WBG semiconductor material and also extreme advancement in fabrication of high quality crystalline SiC has influenced many groups to think over SiC so as to replace Si in the next generations of high power electronic devices. Other advantage of SiC materials is compatible process integration of SiC devices with Si based devise allows use of the same technology required for Si. Therefore it is important to discuss material and electrical properties of SiC and compare them with Si.

1.2 SiC Structure

In this section we will discuss SiC's crystalline structure and its polytypic nature. The influence of polytypism on the physical properties of SiC is also presented.

SiC is a group IV compound semiconductor. The main building block of the semiconductor material is a tetrahedron of C (Si) atom at the centre covalently bonded to four Si (C) atoms. The distance between two neighbouring Si or C atoms is 3.08 Å approximately and the distance between each pair of Si atom and C atom (i.e. Si-C bond length) is almost equal to 1.89 Å [1].

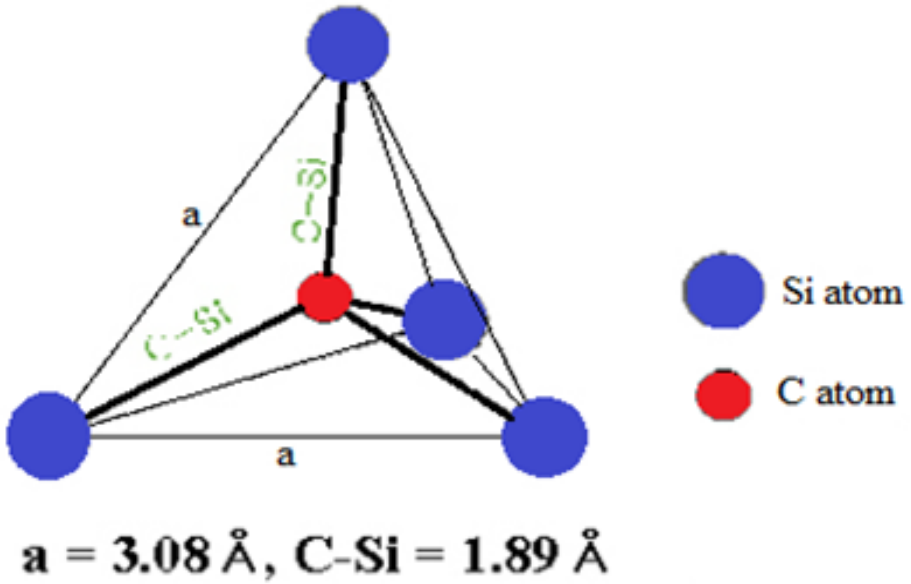

Figure 1.1: Si-C tetrahedral basic unit [1]

1.2.1 SiC Polytypes

Silicon carbide is a wide band gap semiconductor with an energy gap wider than 2eV (E_g>2eV). It can be crystallized in a number of polytypes (a one dimension-type polymorphism). Polytypes differ for the stacking sequence of atomic layer along one crystalline direction.

The basic units of SiC are periodically repeated in closed-packed hexagonal layers, whose stacking sequence gives rise to the different polytypes. Though being different in the long range order, the several polytypes show a similar local

chemical environment for both the carbon and silicon species; in particular each C (Si) atom is situated above the centre of a triangle of Si(C) atoms and underneath a Si(C) atom belonging to the next layer in a tetrahedral coordination. The distance between neighbouring silicon or carbon atoms and Si-C bond length remains same for all polytypes.

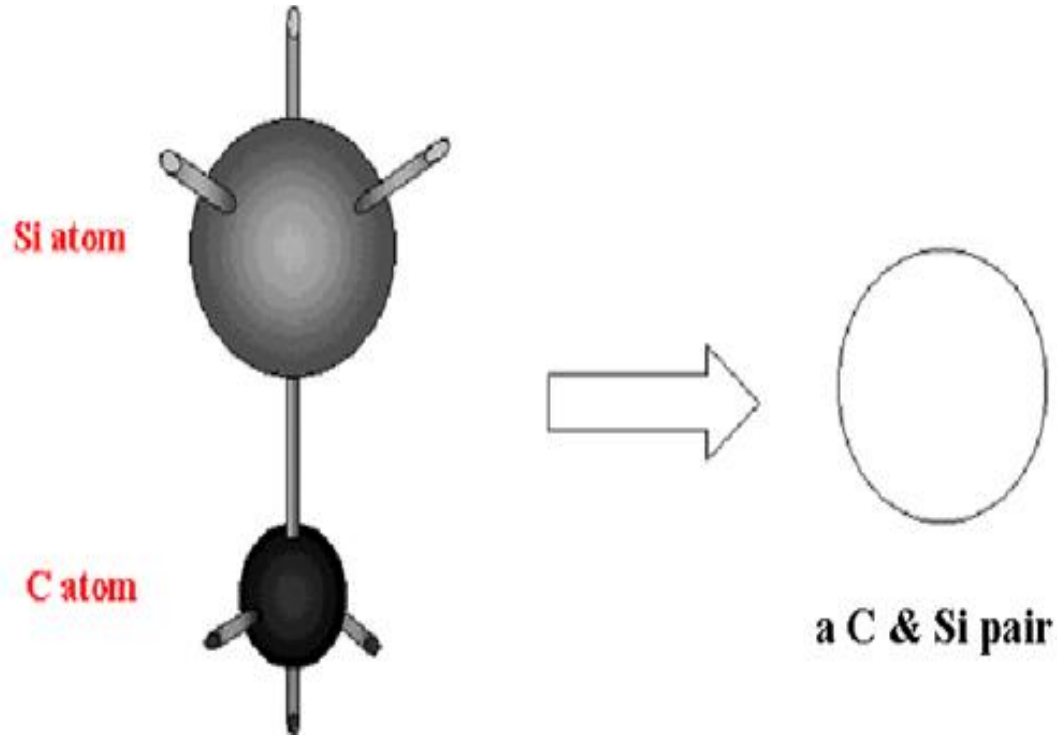

Figure 1.2: Visual image of SiC bonding [2]

SiC crystallizes in close packed structures consisting of bi-layers of Si and C atoms. One Si-C bi-layer consists of one building block which can occupy three different positions denoted A, B or C. Starting from a layer where atoms are in position A, the other layer can be stacked in position B or C. If the sequence starts with layer B, the next layer can occupy position A or C. Close packing structure of SiC spheres are shown in Figure 1.3. Figure 1.3.1shows the 1st layer, “A”, formed by placing spheres in the crevice of the adjoining row. Figure 1.3.2 shows the 2nd layer, "B", formed by placing spheres in a hollow on top of the 1st layer. On x and y site hollows on top of the 2nd layer, two types of arrangement of spheres are possible for the 3rd layer, “C”.

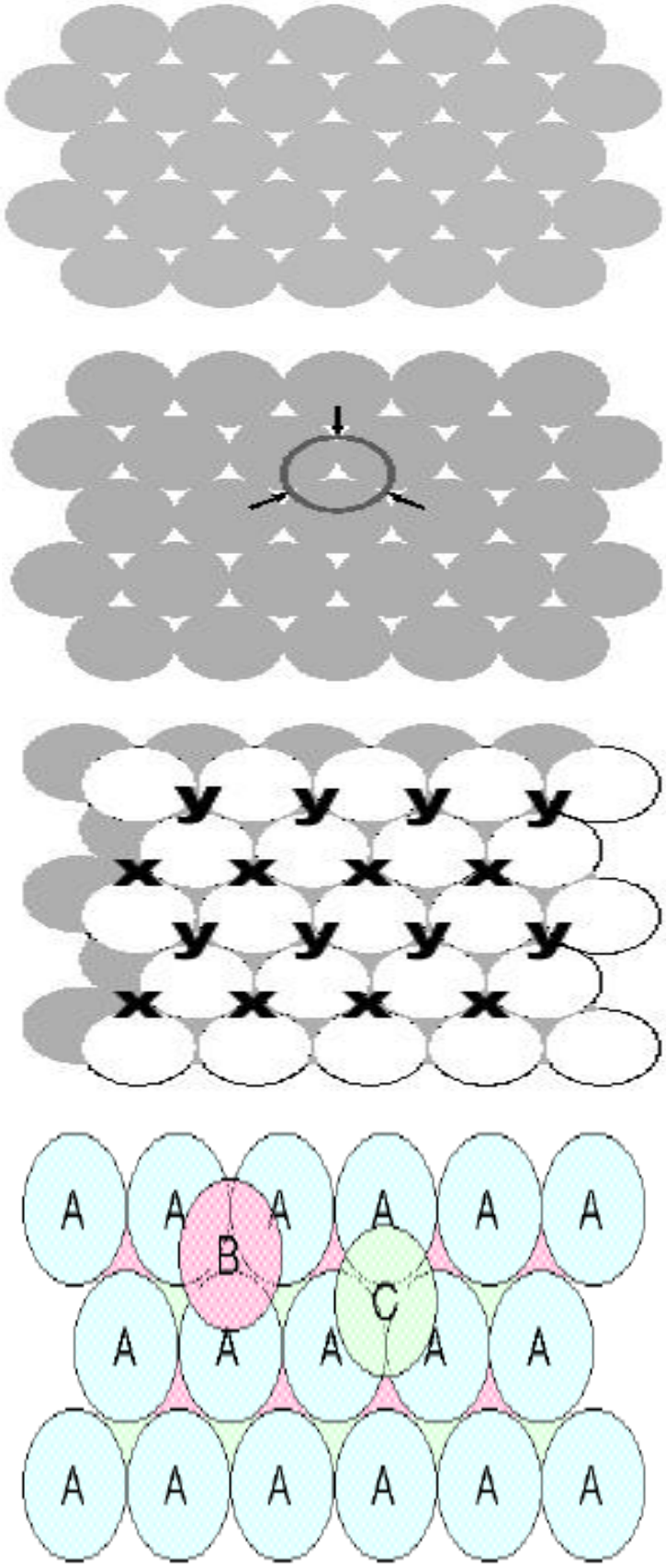

Figure 1.3: Close packing structure of SiC spheres [2]

Due to different stacking order of silicon and carbon atoms, silicon carbide undergoes a variety of crystal structures although the chemical composition is the same. This characteristic which is known as polytypism has brought a number of polytypes for SiC crystalline structure. The number of atoms in unit cell varies from polytype to polytype and its physical and electrical properties are varied accordingly. To date, SiC has more than 200 polytypes [3]. Among these, there is only one cubic polytype β-SiC or 3C-SiC. All the rest are α-SiC. 3C-, 4H- and 6H-SiC are three stable single crystalline polytypes for device purposes.

If we designate a Si-C atom pair in an A-plane in a close packed lattice as A, and in the B-plane as B, and in the C-plane as C, then we can generate a series of lattice unit cells by variation of SiC plane stacking sequence along the principal crystal axis as in Figure 1.4. For example the cubic polytype (β-SiC or 3C-SiC) presents a stacking sequence ABCABC [4], which is typical of a zincblende structure. ABAB... stacking, will generate the 2H-SiC wurtzite lattice. Other stacking sequences, such as ABCB… will generate 4H-SiC; ABCACB... will generate 6H-SiC; ABCACBCABACABCB… will generate 15R-SiC.

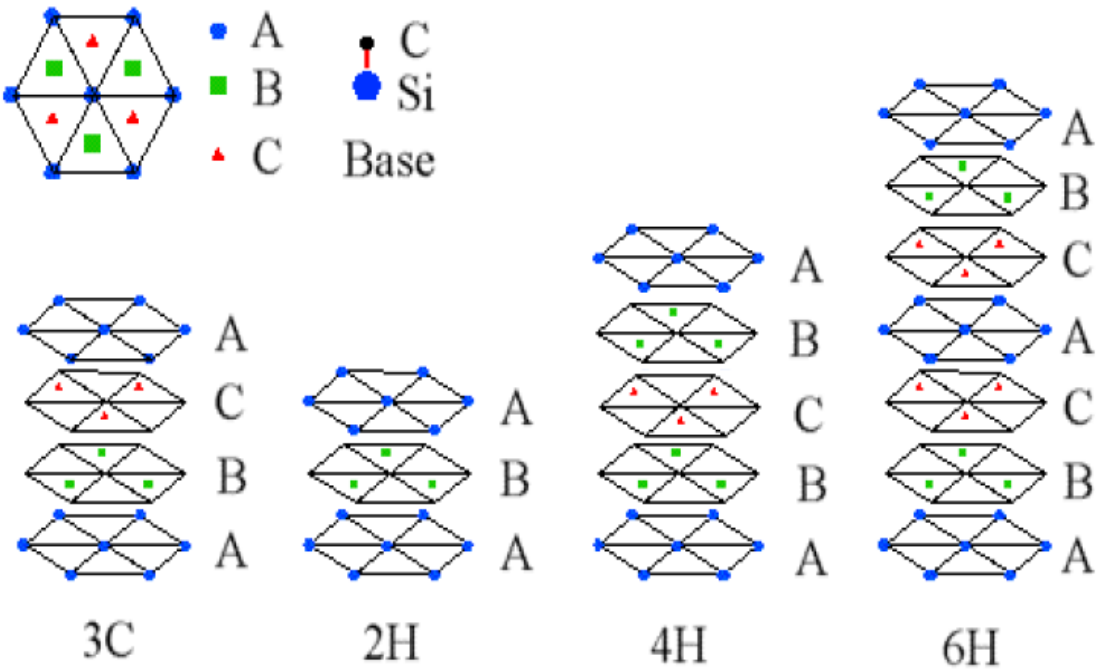

Figure 1.4: Stacking sequences of SiC polytypes [5]

These SiC polytypes are represented in the Ramsdell notation [6]. In this representation the digit in the name is the number of double layers (one Si and one C layer) in the primitive lattice cell; the character gives the type of crystal symmetry. H stands for hexagonal, C for cubic and R for rhombohedral.

The number of atoms per unit cell varies from polytype to polytype, significantly affecting the number of electronic energy bands and vibrational branches possible for a given polytype. This diversity in electronic and vibrational band structures tremendously affects the physical properties of the different polytypes.

1.2.1.1 2H-SiC

The substrate of 2H-SiC is not available commercially but small mono-crystalline pieces have been grown [7]. The wurtzite ABAB... stacking sequence is denoted as 2H-SIC reflecting its two bi-layer stacking periodicity and hexagonal symmetry. 2H-SiC's performance in the direction perpendicular to the c-axis is similar to 4H-SiC. Its mobility is better in the parallel to the c-axis direction [8].

1.2.1.2 4H-SiC

The 4H-SiC has a low-field mobility which is about half than that of silicon with a small anisotropy (20% higher in the direction parallel to the c-axis) [9-11]. The anisotropy in 4H-SiC depends on the electric field, and at high electric fields the saturation velocity is 20% lower in the c axis direction. 4H-SiC and 6H-SiC are the most mature polytypes and they have been characterised most thoroughly. 4H-SiC has better transport properties and this polytype forms the basis for most of the commercial products.

1.2.1.3 6H-SiC

As 6H-SiC have a long repetition length in the crystallographic lattice, it has a large anisotropy. The mobility in the direction perpendicular to the c-axis is four times more than that in the c-axis [12]. As compared with silicon 6H-SiC has mobility about 25% in the direction perpendicular to the c-axis, and 7% in the

direction parallel to it. The saturation velocity for 6H-SiC is $2X10^7$ cm/s in the direction perpendicular to the c-axis, but only $0.6X10^7$ cm/s in the direction parallel to it.

1.2.1.4 3C-SiC

The major advantage of 3C-SiC is that it can be grown on silicon substrates. Thus the integration of 3C-SiC devices with the present silicon technology can be made possible in future. There is no stacking faults growth in 3C-SiC. The electron mobility of 3C-SiC is more as compared to that of 4H-SiC but its hole mobility is less. Lower band-gap and breakdown field are the main disadvantages when compared to other polytypes [13].

1.3 Properties of SiC

Considering the several arrangements of Si and C atoms within the SiC crystal lattice, each SiC polytype presents unique fundamental optical and electrical properties since the number of atoms in unit cell changes from polytype to polytype. Electrical properties of 3C-, 4H-, 6H-SiC polytypes are compared in Table 1.1, where properties of Si and GaAs are also stated for reference [14-15]. Properties such as large saturated electronic drift velocity, large breakdown electric field, wide bandgap, small dielectric constant, reasonably high electron mobility and high thermal conductivity has made silicon carbide an acceptable semiconductor for fabricating high power devices with reduced power losses and die sizes. The wide bandgap of SiC compared to Si is considered as the major benefit for high power devices that results in larger critical electric field and higher temperature handling. The high breakdown fields in Silicon Carbide allows drift regions that are eight to ten times thinner than Silicon high voltage devices, with less resistance and lower leakage currents at elevated temperatures for desired breakdown voltage. This makes silicon carbide high power devices practicable even in kilovolt range and beyond. Hence, the improvement in the current handling capability of these devices can be achieved.

The table below compares material properties of Silicon (Si), Silicon Carbide (SiC) and Gallium Nitride (GaN). These material properties have major impact on the performance characteristics of the power devices. Both GaN and SiC have material properties superior to Si for RF and Switching Power devices.

Table 1.1: Comparison of electronic properties of major SiC polytypes, Si and GaAs [16].

Property		Si	GaAs	6H-SiC	4H-SiC	3C-Sic
Band Gap(eV)	E_g	1.1	1.142	3.0	3.26	2.2
Breakdown field (MV/cm)	E_c	0.6	0.6	3.2	3.0	1.5
Electron mobility (cm^2/V-s)*	μ_n	1100	6000	370	800	750
Hole mobility (cm^2/V-s)*	μ_p	420	320	90	115	40
Dielectric constant	ε_r	11.8	12.8	9.7	10	9.6
Saturated electron drift velocity (cm/s)	V_{sat}	10^7	10^7	$2x10^7$	$2x10^7$	$2x10^7$
Intrinsic carrier concentration (cm^{-3})	n_i	$1.5x10^{10}$	$1.9x10^{-10}$	$2.3x10^{-6}$	$8.2x10^{-9}$	6.9
Thermal conductivity (W/cm-K)	λ	1.5	0.5	4.9	4.9	5

*The electron mobility and the hole mobility refer to a doping concentration of about $10^{16}cm^{-3}$ of donors and acceptors respectively.

3C-SiC has the lowest critical electric field and highest electron mobility compared to other polytypes of SiC. This polytype, which is also known as cubic crystalline SiC or β-SiC, has been successfully grown on Si substrate but it still suffers from low material quality. 2-4 inches 4H and 6H-SiC substrates are commercially available today.

The specific on-resistance (R_{on}) of the drift layer can be calculated as:

$$R_{on} = \frac{4V_B^2}{\varepsilon E_c^3 \mu_n}$$

where V_B is the breakdown voltage,

ε is the permittivity in F/cm,

E_c is the breakdown field in V/cm,

μ_n is the electron mobility in cm^2/V-sec

Therefore higher critical electric field in SiC compare to Si not only provides higher breakdown voltage but also results in lower resistance which is required for high power applications.

Band gap

The band gap is a forbidden zone in the energy spectra for a crystal. When the band-gap is large the crystal acts as an insulator and without a band-gap it acts as a metal. A semiconductor has a band-gap up to few eV. The wide energy band gap present in silicon carbide polytypes can be explained considering the very short bond length between Si and C. Both 4H and 6H have a wider band gap than cubic SiC (3.26 eV for 4H vs. 2.2 eV for 3C –SiC) [17].

Critical electric field

Silicon carbide wide band gap implies a high value for the impact ionization energy. This explains because SiC can operate with applied electric fields up to eight times greater than those commonly applied to Si or GaAs, without avalanche breakdown. The breakdown voltage depends not only on the polytype, but also on the direction assumed by the electric field in the material.

This property makes SiC a very good substrate for the fabrication of diodes and transistors operating with high power densities, frequencies and temperatures.

Due to the large band-gap the critical electric field is about eight times higher in SiC than for small band-gap materials, such as Si and GaAs. With high critical electric field devices can be fabricated much smaller for the same voltage, alternatively operate at much higher voltages.

High temperature operation

A high temperature applied to a semiconductor can mean that the number of the created electron – hole pairs is greater than the number of free carriers introduced in the semiconductor with the doping. In these conditions we have an intrinsic semiconductor and SiC becomes intrinsic only at temperatures around 1300 K, with dependence on the polytype and on the doping concentration.

It became clear in the past years that the major issue in the fabrication of high temperature SiC devices was the metal contact failure, so new types of reliable contacts should be developed in order to fully exploit the advantages offered by the high intrinsic temperature of SiC.

Optical properties as related to energy band gap

The band gap of SiC is indirect and optically efficient devices (such as LEDs) cannot be fabricated. However, the SiC wide band gap can be advantageously applied in optical detectors for the UV region of the electromagnetic spectrum.

Saturated electron drift velocity

At high electric fields the velocity ceases to be proportional to the electric field, due to increased scattering. Saturation velocity is the maximum velocity a charge carrier in a semiconductor can attain in the presence of high electric fields. The value of saturated electron drift velocity for silicon carbide is approximately twice the value that for silicon. Higher saturation velocity allows faster devices with shorter switching times.

Carrier density and mobility

The leakage current in SiC devices such as Schottky diodes can be kept low, due to the semiconductor small intrinsic carrier concentration. This is an advantage especially when high temperature devices are considered. The term carrier mobility refers to both electron mobility and hole mobility. SiC shows increasing values for the carrier mobility when the applied electric field increases, while Si and GaAs in the same condition behave differently. In particular, Si shows an early saturation of the carrier velocity, whilst GaAs is characterized by a peak in the carrier mobility followed by a sharp decrease to a value very close to those reported for Si.

Thermal conductivity

Thermal conductivity is a quality that is very important in power semiconductor devices in order to transport the heat in the device. The high values of the silicon carbide thermal conductivity (λ) can permit to the devices to operate with higher power densities than Si or GaAs. When the effect of the higher critical field is considered, the following relation for the temperature increase ΔT across a junction can be introduced:

$\Delta T = \theta\, t/\lambda$, where θ is the thermal flow and t is the device thickness.

We can see that a high junction operating temperature is common for SiC devices, especially when small dimension are taken into account. A good choice of the solder mounted on the chip must be then considered, in order to avoid problems related to the heat dissipation.

1.4 Advantages and Applications of SiC Electronics

Silicon carbide is the only WBG semiconductor that possesses a high-quality native oxide suitable for use as an MOS insulator in electronic devices. Thermal oxidation of SiC produces a layer of SiO_2 on the surface, while the carbon atoms

from the SiC form CO, which escapes as a gas. Thus it is possible to make all the devices found in silicon IC technology in SiC, including high quality, stable MOS transistors and MOS integrated circuits.

Silicon carbide contributes most valuable advantage in the areas of high temperature and high power device operations.

As the SiC has low intrinsic carrier concentration and wide bandgap energy, it allows SiC to maintain semiconductor behaviour at much higher temperatures than silicon, which in turn permits SiC semiconductor device performance at much higher temperature than silicon [18]. As temperature increases, intrinsic carriers increase exponentially so that undesired leakage currents grow unacceptably large, and eventually at still higher temperatures, the semiconductor device operation is overcome by uncontrolled conductivity as intrinsic carriers exceed intentional device dopings [19, 20]. Depending upon specific device design, the intrinsic carrier concentration of silicon generally confines silicon device operation to junction temperatures <300 ^{o}C. SiC's much smaller intrinsic carrier concentrations theoretically permit device operation at junction temperatures exceeding 800 ^{o}C.

The ability to place uncooled high-temperature semiconductor electronics directly into hot environments would enable important benefits to automotive, aerospace, and deep-well drilling industries [18, 21]. High temperature capability eliminates performance, reliability, and weight penalties associated with liquid cooling, fans, thermal shielding, and longer wire runs needed to realize similar working in engines using conventional silicon semiconductor electronics.

The high breakdown field and high thermal conductivity of SiC along with high operational junction temperatures theoretically permit high power densities and efficiencies to be realized in SiC devices. The breakdown field in SiC is about 8 times higher than in silicon. This is important for high-voltage power switching transistors. This enables the blocking voltage region of a power device to be

roughly ten times thinner and ten times heavily doped, resulting in approximately 100-fold beneficial decrease in the blocking region resistance at the same voltage rating [22]. The fact that high voltage operation is achieved with much thinner blocking regions using SiC enables much faster switching in both unipolar and bipolar power device structures. Therefore, SiC based power converters could operate at higher switching frequencies with much greater efficiency (i.e. less switching energy loss) [23, 24].

Table 1.2: Major SiC advantages and some applications

	SiC advantages	Applications
Electrical Properties	Wide bandgap Larger electric field High saturated electron drift velocity	High temperature electronics and sensors Power devices UV and radiation detectors High frequency devices
Chemical Properties	Biocompatibility Inertness	Bio-sensors Chemical sensors
Mechanical Properties	Young modulus Hardness	Mechanical sensors Surface coating Disc brakes and clutch
Thermal Properties	High thermal conductivity	Power devices

Uncooled operation of high temperature and high power SiC electronics would enable revolutionary improvements to aerospace systems [18]. SiC high power solid-state switches will also enable large efficiency gains in electric power management and control [23]. More efficient electric motor drives enabled by SiC will also benefit industrial production systems as well as transportation systems

such as diesel-electric railroad locomotives, nuclear powered ships, and electric automobiles and buses.

The mechanical properties such as hardness, high Young's modulus and low friction coefficient makes SiC a favourable material for applications other than electronics. Like disc brakes and clutch made of silicon carbide has been used on some sport cars. Table 1.2 lists the various applications of silicon carbide.

CHAPTER 2

Power Semiconductor Devices

Power semiconductor device has played an essential role in the development of power electronics as its key system topologies. Compared to normal electronic devices, power semiconductor devices require large voltages in the off state and high current capability in the on state, which demand geometry differences from the low-power devices.

Since 40 years, power semiconductors have been playing leading role in the progress of power electronics, because they are essential to satisfy the constantly growing demands on cost, performance and reliability. Power semiconductor devices first appeared in 1952 with the introduction of the power diode by R.N. Hall. It was made of Ge and had a voltage capability of 200 V. They started to play their principal role to the transition from germanium to silicon and in the field of high-power devices to that of the float zone and neutron transmutation doped FZ NTD.

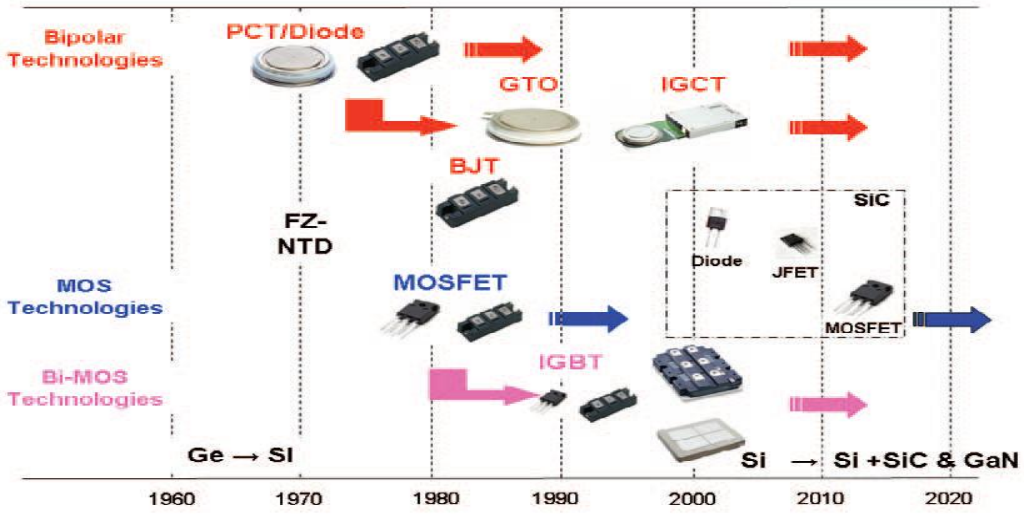

Figure 2.1: The evolution of power devices [26]

Most of the time, they have been drawing experience from progresses in the technology of integrated circuits (ICs) [25]. Since very early, the ICs have represented the edge of development, and contrary to power devices and systems, they have been considered as "high-tech". Power devices and systems are becoming high-tech. They have to combine a bundle of modern technologies to satisfy harder demands than ever before. As the demand for electricity is growing fast in all parts of the world, its generation has to increase. It is clear that power semiconductors are the key enablers of this progress thanks to the already existing device concepts and technologies [26].

2.1 Common Power Devices

Power semiconductor device can be divided into two main categories based on terminal numbers:

- 2-terminal devices (diodes), whose state is completely dependent on the external power circuit they are connected to; and
- 3-terminal devices, whose state is not only dependent on their external power circuit, but also on the signal on their driving terminal (gate or base). Transistors or thyristors belong to this category.

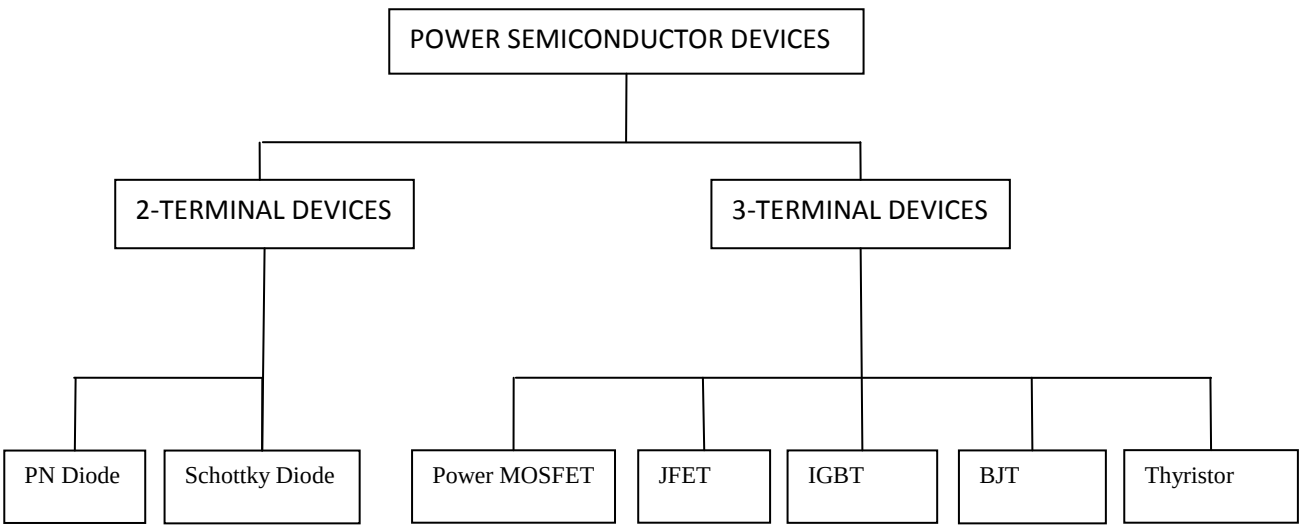

Figure 2.2: Power Semiconductor Devices [27]

A second classification is less obvious, but has a strong influence on device performance. Some devices are majority carrier devices (Schottky diode, MOSFET), while the others are minority carrier devices (Thyristor, bipolar transistor, IGBT). The former uses only one type of charge carriers, while the latter use both (i.e. electrons and holes). The majority carrier devices are faster, but the charge injection of minority carrier devices allows for better On-state performance.

The thyristors appeared in 1957. Thyristors are able to withstand very high reverse breakdown voltage and are also capable of carrying high current. One disadvantage of the thyristor for switching circuits is that once it is 'latched-on' in the conducting state it cannot be turned off by external control. The thyristor turn-off is passive, i.e., the power must be disconnected from the device.

The first bipolar transistor devices with substantial power handling capability were introduced in the 1960s. These components overcame some limitations of the thyristors because they can be turned on and off with an applied signal.

With the improvements of the MOS technology, power MOSFETs became available in the late 1970s. These devices allow operation at higher frequency than bipolar transistors.

The Insulated Gate Bipolar Transistor (IGBT) developed in the 1980s became widely available in the 1990s. This component has the power handling capacity of the bipolar transistor, with the advantages of the isolated gate drive of the power MOSFET.

2.2 Schottky Barrier Diode

SiC Schottky Barrier diodes (SBDs) or metal-semiconductor diodes are attractive since they provide rectification without significant switching loss. Switching loss occurs when a diode change from the conducting state to the blocking state [20, 27]. Schottky diodes are metal-semiconductor junctions, and conduction current in these devices consists only of electrons injected from the n-type semiconductor into the metal. Since no holes are injected into the semiconductor, there is no stored charge and no reverse recovery transient, so the SBD turns off very rapidly. The reverse current transient of the diode causes power dissipation in other components of the switching system, typically a switching transistor, and this switching loss is attributed to the diode since the current transient is caused by the diode. Substitution of a p-i-n diode by a SBD effectively eliminates the switching loss.

Although Schottky diodes are desirable because of their low switching loss, it is not feasible to build high voltage SBDs in silicon. This is because of the relatively low barrier heights between common metals and silicon. The bandgap energy of silicon is 1.12 eV and the barrier heights of metal contacts to silicon are typically less than 0.5 eV. Under large reverse bias, the barrier is further reduced by Schottky barrier voltages. This is not the case with SiC because it is easy to fabricate SBDs with barrier heights as high as 1.5 eV. Since the reverse current depends exponentially on the barrier height, the reverse leakage in SiC SBDs is orders of magnitude lower than in silicon, even at high voltages [28].

The structure of a metal-semiconductor junction is shown in Figure 2.3. It consists of a metal in contact with piece of semiconductor. Metal- semiconductor junctions are of two types: rectifying and non-rectifying. Rectifying junction forms the Schottky barrier whereas non-rectifying junction forms the ohmic contact. In an ideal ohmic contact, no potential is present between the metal and the semiconductor.

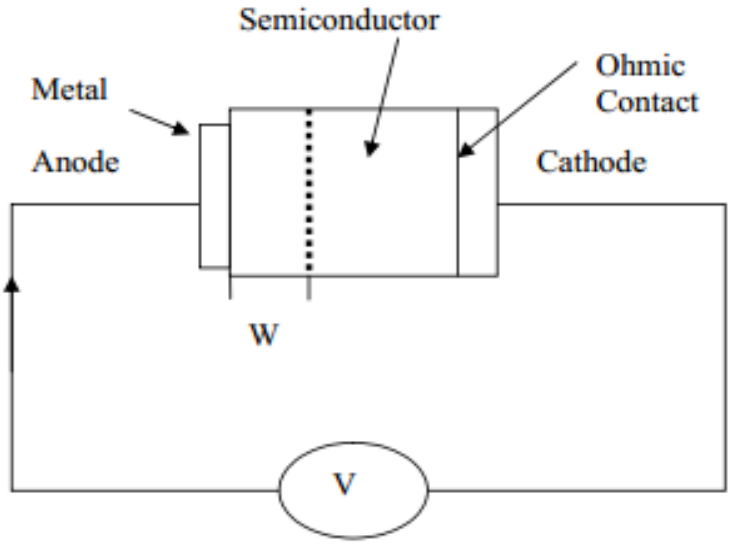

Figure 2.3: Structure of metal-semiconductor junction [29]

2.2.1 Schottky Barrier Formation

The formation of an ideal Schottky contact depends on the work functions of the two materials i.e. metal and the semiconductor being brought into contact with each other. When a metal and a semiconductor are brought into contact, either a Schottky contact or an Ohmic contact can be formed depending on the characteristics of the interface. Both of these contacts are highly important for solid state research. The type of the contact form is determined by the difference between the metal and the semiconductor work functions. Work function of a metal is the energy required to knock a valence electron from the metal into the free space or vacuum. It is often measured through the use of the photoelectric effect. The metal's work function Φ_m is an intrinsic property and is constant assuming there is no worry of depleting the valence electrons; in other words, there are a lot of metal atoms. Thus, the metal work function Φ_m can be described as vacuum level, E_o, subtracted from the energy level where the valence electrons sit, which is known as metal's Fermi level, E_{fm}.

$$\Phi_m = E_o - E_{fm} \tag{2.1}$$

Work function of semiconductor Φs can be given as:

$$\Phi_s = \chi + (E_C - E_{fs})_{FB} \quad (2.2)$$

where χ is known as the semiconductor electron affinity and is an invariant property of the semiconductor, E_{fs} is the semiconductor Fermi level with $(E_C - E_{fs})_{FB}$ the difference between conduction band edge and semiconductor Fermi level under flat band conditions. The equilibrium position of the Fermi level in the semiconductor is not an invariant value. It is positioned based on conductivity type and doping concentration meaning that $(E_C - E_{fs})_{FB}$ can be varied. This means that unlike the metal work function, the semiconductor's work function can be varied.

When a metal and a semiconductor are brought in contact, the respective Fermi-levels must coincide in thermal equilibrium as shown in Figure 2.4(b). There are two limiting cases, one is the ideal case referred to as Schottky-Mott limit [30] and other is the practical case referred to as the Bardeen limit [31]. Figure 2.4 shows the energy band diagram for the ideal case i.e. Schottky-Mott limit with the absence of surface states.

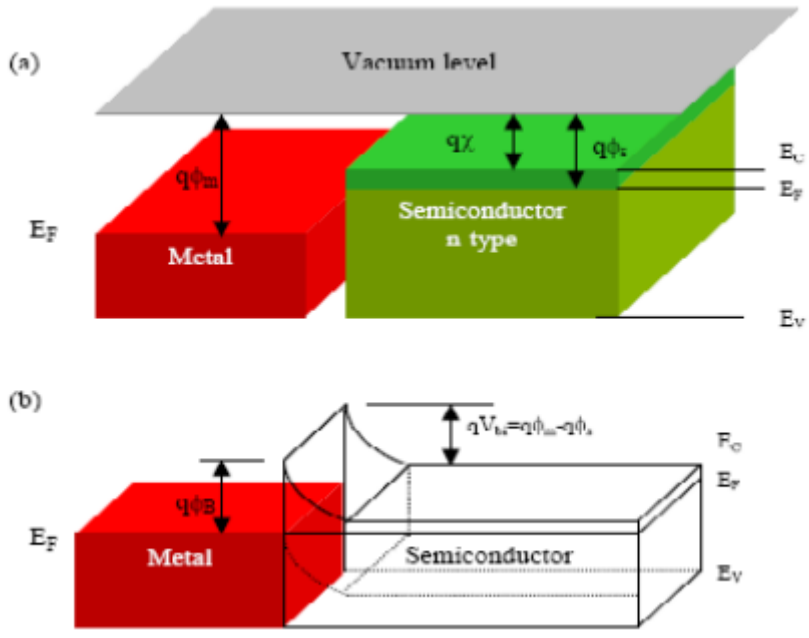

Figure 2.4: Metal and semiconductor barrier formation (a) Neutral and isolated and (b) In perfect contact without any oxide between them [30]

In this case the barrier height Φ_{Bn} for n-type semiconductor can simply be calculated as the difference between the metal work function Φ_m and electron affinity of the semiconductor:

$$q\,\Phi_{Bn} = q(\,\Phi_m - \chi_s\,) \tag{2.3}$$

For a given semiconductor and a metal, the sum of the barrier heights Φ_{Bn} of the n-type and Φ_{Bp} of the p-type semiconductor results to be equal to the energy bandgap:

$$q(\,\Phi_{Bn} + \Phi_{Bp}\,) = E_G \tag{2.4}$$

This relationship for Schottky-Mott limit implies that the control of the barrier height is achieved by the choice of the metal. The second limiting case is the Bardeen limit where a large density of states is present at the semiconductor to metal interface. In the Bardeen limit the barrier height Φ_B is completely independent of the metal work function Φ_m in contrast to the Schottky-Mott limit and the Fermi level is said to be pinned by the high density of interface states.

The Fermi levels of the two dissimilar materials do not match when the vacuum levels of the material are set equal. The instant the metal and semiconductor are made in contact with each other, their Fermi levels still do not align. However, a

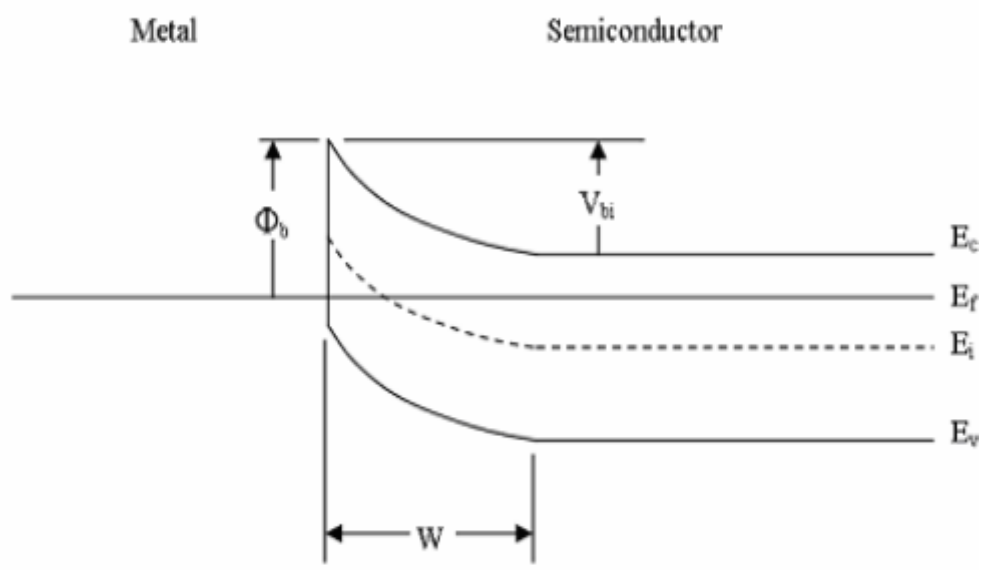

Figure 2.5: Energy band diagram of Schottky contact at equilibrium [30]

splitting in Fermi levels signifies non-equilibrium conditions exist. This is obviously not the case since no external perturbation is being applied. Therefore, to get the equilibrium conditions, transference of electrons between the semiconductor and the metal will occur. This will result in depletion region at the interface of the semiconductor and the metal. At equilibrium, the Fermi level is invariant with position as shown in Figure 2.5.

Metal- semiconductor contact can either be rectifying or non-rectifying depending on the difference between work function of the metal and the semiconductor. The conditions for rectifying and non-rectifying contacts are given in Table 2.1 below.

Table 2.1: Metal-semiconductor contact type

	n-type	p-type
$\Phi_m > \Phi_s$	Rectifying(Schottky)	Non-rectifying(Ohmic)
$\Phi_m > \Phi_s$	Non-rectifying(Ohmic)	Rectifying(Schottky)

The rectifying contact has a built-in potential, V_{bi} that can be equated from the Schottky barrier height and semiconductor doping level as

$$V_{bi} = \frac{1}{q}[\Phi_b - (E_C - E_{fs})_{FB}] \tag{2.5}$$

where $\Phi_b = \Phi_m - \chi$ is the Schottky barrier height and q is the charge on an electron. Using one sided abrupt junction, such as those used for p^+-n junctions, the usual electrostatic variables can be obtained for non-punch through devices.

$$\text{Electric field, } E(x) = \frac{-qN_d}{K_s \in_o}(W - x), \tag{2.6}$$

$$\text{Voltage, } V(x) = \frac{-qN_d}{2K_s \in_o}(W - x)^2, \tag{2.7}$$

$$\text{Depletion Width, } W = \sqrt{\frac{2K_s \in_o}{-qN_d}(V_{bi} - V_a)} \tag{2.8}$$

where N_d is the doping of the semiconductor,

K_s is the permittivity of the semiconductor,

$\in_o$ is the permittivity of free space,

V_a is the voltage applied to the Schottky contact and

x is the distance drom the metal-semiconductor interface

2.2.2 Schottky Barrier Diode Structure

The cross sectional view of a typical Schottky Barrier diode in SiC is shown in Figure 2.6. A lightly doped n-type blocking layer is grown by chemical vapour deposition on a SiC substrate. The doping and thickness of the epilayer are so selected so as to achieve the desired blocking voltage [28].

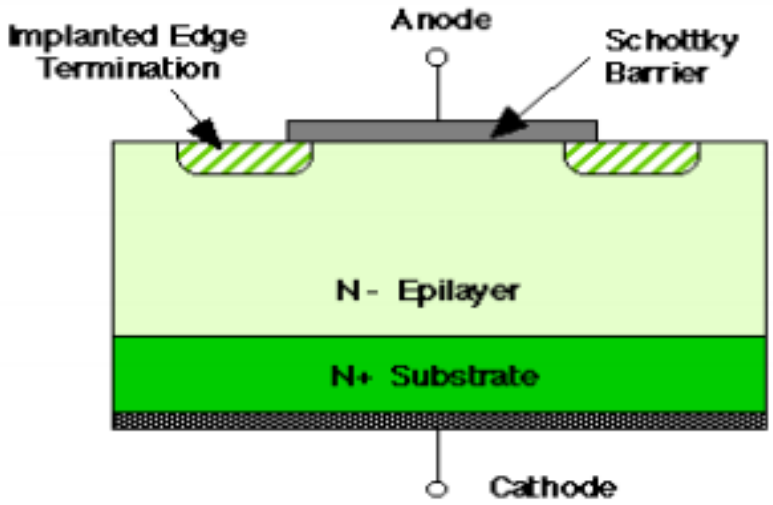

Figure 2.6: Cross section of the Schottky Barrier diode in SiC [32]

The Schottky junction on the top surface of the blocking layer is formed by implanting an edge termination ring at the surface, then depositing the Schottky metal. The edge termination ring is needed to prevent field crowding at the

periphery of the metal in the blocking state; otherwise there would be significant reduction in the blocking voltage. Two types of edge termination rings have been used, one is resistive termination extension (RTE) and other is junction termination extension (JTE).

2.3 Literature Survey

It was in 1938 that German physicist Walter H. Schottky created a theory that illustrated the rectifying behaviour of a metal-semiconductor contact as dependent on a barrier layer at the surface of contact between the two materials. The metal semiconductor diodes i.e. Schottky Barrier diodes are later fabricated on the basis of this theory. Eventually after an endless research and development has been in advancement in this field. In March 1993, Mohit Bhatnagar and B.J. Baliga showed theoretically that an ideal SiC Schottky rectifier can provide a breakdown voltage as high as 5000V with a forward voltage drop of only 3.85V at 300°K for a current density of 100Amps/cm^2. R. Raghunathan in 1995 showed for the first time that breakdown voltage of 1000V can be achieved for 4H-SiC Schottky Barrier diode. In June 1995, Akhira Itoh et al. showed that high performance of high-voltage rectifiers could be realized using 4H-SiC Schottky Barrier diodes. A typical breakdown voltage of 800V could be achieved [33]. Akhira Itoh et al. showed in 1996 that using highly resistive layers formed by B^+-edge termination can help in improving the reverse blocking characteristics of 4H-SiC Schottky rectifiers [34].

In 1997, the results obtained with limited area amorphisation by argon ion-implementation at the periphery of 6H-SiC Schottky Barrier diodes were reported [35]. A variety of edge termination structures based upon the amorphised implanted region were studied. The termination structures were fabricated using a three-mask process to create a high resistivity layer at the periphery of the device formed by using high dose argon ion-implantation with its position and area defined using a photoresist mask. It was established that, for obtaining a high breakdown voltage, the high resistivity layer should be in contact with the

Schottky metal. It was demonstrated that only 50 μm of the implant region is required at the periphery to obtain ideal plane parallel breakdown voltages.

In June15, 1998, Hitachi announced the release of Schottky Barrier diode, the HSB0104YP containing two diode elements. This new product made possible high speed switching at the pico-second level. It has a reverse voltage of 40V. ROHM developed the "ROBOSIL-40" Schottky Barrier diode with an ultra low forward voltage with Backward voltage of 40V, providing an extremely low forward voltage of only 0.29V. In July 1998, Purdue University reported, 4H-SiC SBD's using both Ni & Ti as Schottky metals. These diodes have been fabricated, which have reverse-blocking voltages of 1720V and 1480V respectively. In 1999, V.K Saxena et al. fabricated 1kV 4H and 6H-SiC Schottky diodes utilizing a metal oxide overlap structure for electrical field termination. The same year, Purdue University group fabricated Ni-Schottky diodes on a 50μm epilayer of 4H–SiC. These diodes exhibited blocking voltages as high as 4.9kV. In 2001, models for the electron mobility in 4H, 6H, and 3C-SiC were explained in a paper by Matthias et.al. [36]. A number of experimental mobility data and Monte Carlo (MC) results reported in the literature have been evaluated and serve as the basis for model development. The proposed models describe the dependence of the electron mobility on doping concentration, temperature and electric field.

Royal Institute of Technology, Department of Microelectronics & IT, Stockholm, reported in 2002 that Schottky rectifiers in SiC are candidates to replace Si-PIN diodes in 300-3000V blocking voltage range. Nuremberg, Germany, 14th May, 2002, Dynex Semiconductors Ltd, a leading power semiconductor company announced that the company has been awarded a research & development grant in a new Program (ESCAPEE) to develop 3.3KV Schottky Barrier diode technology from SiC. Marinsz et. al. showed the result of investigation of the forward and reverse current-voltage(I-V) characteristics of 4H-SiC Schottky rectifiers with Nickel as the contact metal [37]. In 2003, P.Tobias et.al. showed that Metal-Insulator–Silicon Carbide devices can be used for gas sensing in automotive

exhausts, because the large band gap of silicon carbide allows high temperature operation. Researchers at the Silicon Carbide lab of Rutgers University in New Jersey, demonstrated 1.79KV, 6.6A 4H-SiC merged PIN-Schottky diodes in 2004.

In 2005, the performance of the commercially available and recently fabricated Schottky Barrier Diode of breakdown voltage of 1.2 kV was compared with the Si diodes at high temperature [38]. It was found that for a rated breakdown voltage of 1.2 kV, SiC Schottky diodes offer better performances in terms of switching time and recovery charge than PN-Si ultra-fast diodes, although they show slightly higher forward voltage drops. Lower reverse leakage current was obtained using Ni instead of Ti for the Schottky contact.

In 2006, Silicon Carbide as energy efficient wide band gap device was discussed [39], which showed that SiC Schottky diodes allowed up to a 25% reduction in losses in power supplies for computers and servers when used in the power factor correction circuit. For motor control, SiC Schottky allowed a >35% reduction in losses as demonstrated for a 3HP motor drive.

In 2007 Electrical and Computer Engineering Department , Purdue University, put up the analysis of Schottky and PIN Diodes on epitaxial 4H-SiC wafers. In 2009, a method to theoretically calculate current-voltage characteristics of Schottky barrier diode defined by the diode equation was given, using iteration method and C++ programming. The diode equation is split into two functions. A set of values of current and voltages was generated using C++ program. The analysis has been made using 4H-SiC diode with contacts of Nickel, Titanium & Gold [40].

In 2012 HOYA Corporation has succeeded in raising the SiC growth rate to more than 50 times the conventional rate, using a newly developed SiC fabrication process. With this new process, large monocrystal 3C-SiC substrates (at least 200 micro-meters thick after removing the Si base layer) can be manufactured. These can then be handled using the same processes that are applicable to conventional Si substrates. Thus, HOYA's 3C-SiC substrate has the same geometry as typical Si

wafers, and can be used in conventional Si semiconductor device production lines without hardware modifications [41].

In 2013 a novel direct wafer bonding technique has been reported; Si wafers to polycrystalline silicon carbide carrier wafers. The purpose of this work is to provide a platform for 3C-SiC epitaxial growth above the wafer bonded Si wafers. 3C-SiC epitaxial layers have been grown by conventional chemical vapour deposition techniques above Si/SiC structures. All of these 3C-SiC epitaxial layers are highly crystalline in nature [42].

CHAPTER 3

Theoretical Analysis

The commercial doping profiles used in the semiconductor devices are usually non-linear either Gaussian profile or complementary error function profile (erfc). Here complimentary error function profile has been used for evaluating the device breakdown voltages. The erfc generalized function can be expressed as:

$$E_n(x) = \frac{n!}{\sqrt{\pi}} \int_0^x e^{-t^n}\, dt \qquad \text{, where n= 1, 2 and 3} \tag{3.1}$$

$$\text{Also,} \quad E_n(h-x) = \frac{n!}{\sqrt{\pi}} \int_0^{h-x} e^{-t^n}\, dt \tag{3.2}$$

On integrating, the expression for $E_n(h\text{-}x)$ comes out to be:

$$E_n(h-x) = \frac{n!}{\sqrt{\pi}}\left[(h-x) - \frac{(h-x)^{n+1}}{n+1} + \frac{(h-x)^{2n+1}}{2(2n+1)} - \frac{(h-x)^{3n+1}}{6(3n+1)} + \cdots\right] \tag{3.3}$$

This gives three erfc functions:

For, n=1

$$E_1(h-x) = \frac{1}{\sqrt{\pi}}\left[(h-x) - \frac{(h-x)^2}{2} + \frac{(h-x)^3}{6} - \ \ldots\ldots\right] \tag{3.4}$$

Complementary error function is given by

$$\text{erfc}_1(h-x) = 1 - E_1(h-x)$$

$$= 1 - \frac{1}{\sqrt{\pi}}\left[(h-x) - \frac{(h-x)^2}{2} + \frac{(h-x)^3}{6} - \ \ldots\ldots\right] \tag{3.5}$$

For, n=2

$$E_2(h-x) = \frac{2}{\sqrt{\pi}}\left[(h-x) - \frac{(h-x)^3}{3} + \frac{(h-x)^5}{10} - \ldots\ldots\right] \quad (3.6)$$

Complementary error function is given by

$$erfc_2(h-x) = 1 - E_2(h-x)$$

$$= 1 - \frac{2}{\sqrt{\pi}}\left[(h-x) - \frac{(h-x)^3}{3} + \frac{(h-x)^5}{10} - \ldots\ldots\right] \quad (3.7)$$

For, n=3

$$E_3(h-x) = \frac{6}{\sqrt{\pi}}\left[(h-x) - \frac{(h-x)^4}{4} + \frac{(h-x)^7}{14} - \ldots\ldots\right] \quad (3.8)$$

Complementary error function is given by

$$erfc_3(h-x) = 1 - E_3(h-x)$$

$$= 1 - \frac{6}{\sqrt{\pi}}\left[(h-x) - \frac{(h-x)^4}{4} + \frac{(h-x)^7}{14} - \ldots\ldots\right] \quad (3.9)$$

Doping Profile

The doping profile used here in Schottky Barrier diode is a complementary error function with different values of constants i.e. n=1, 2 and 3. This constant has been used just to vary the gradient of the profile. The carrier concentration is maximum at the base of the device decreasing upwards at the contact. The equation to this profile may be written as:

$N(x) = N_O \times erfc_n(h-x)$, where N_O is the peak carrier concentration (3.10)

For, n=1

$$N(x) = N_0\left[1 - \frac{1}{\sqrt{\pi}}\left\{(h-x) - \frac{(h-x)^2}{2} + \frac{(h-x)^3}{6} - \ldots\ldots\right\}\right] \quad (3.11)$$

For, n=2

$$N(x) = N_0\left[1 - \frac{2}{\sqrt{\pi}}\left\{(h-x) - \frac{(h-x)^3}{3} + \frac{(h-x)^5}{10} - \ldots\ldots\right\}\right] \quad (3.12)$$

For, n=3

$$N(x) = No\left[1 - \frac{6}{\sqrt{\pi}}\left\{(h-x) - \frac{(h-x)^4}{4} + \frac{(h-x)^7}{14} - \ldots\ldots\right\}\right] \quad (3.13)$$

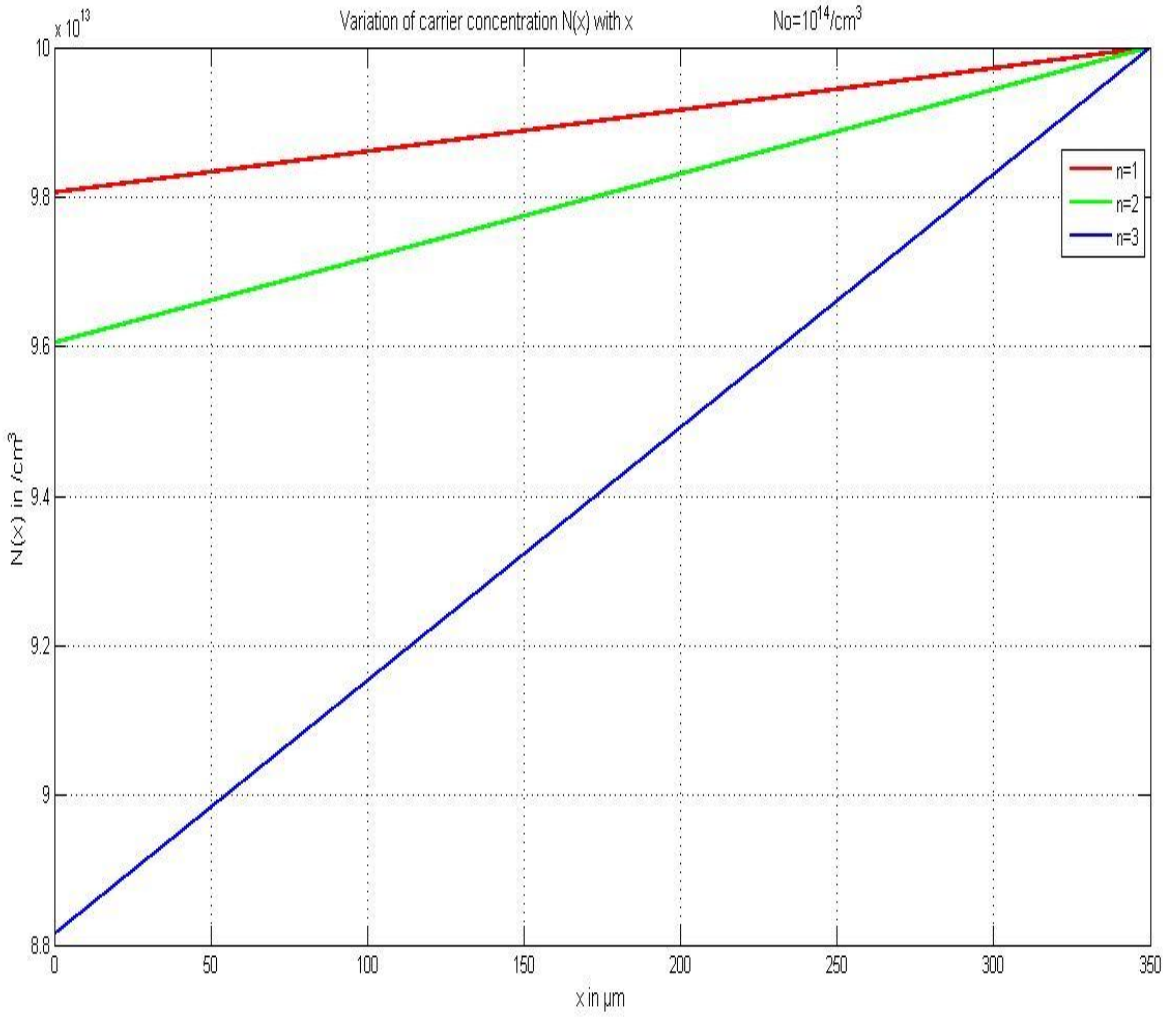

Figure 3.1 Variation of carrier concentration N(x) with x with peak concentration 10^{14} /cm^3.

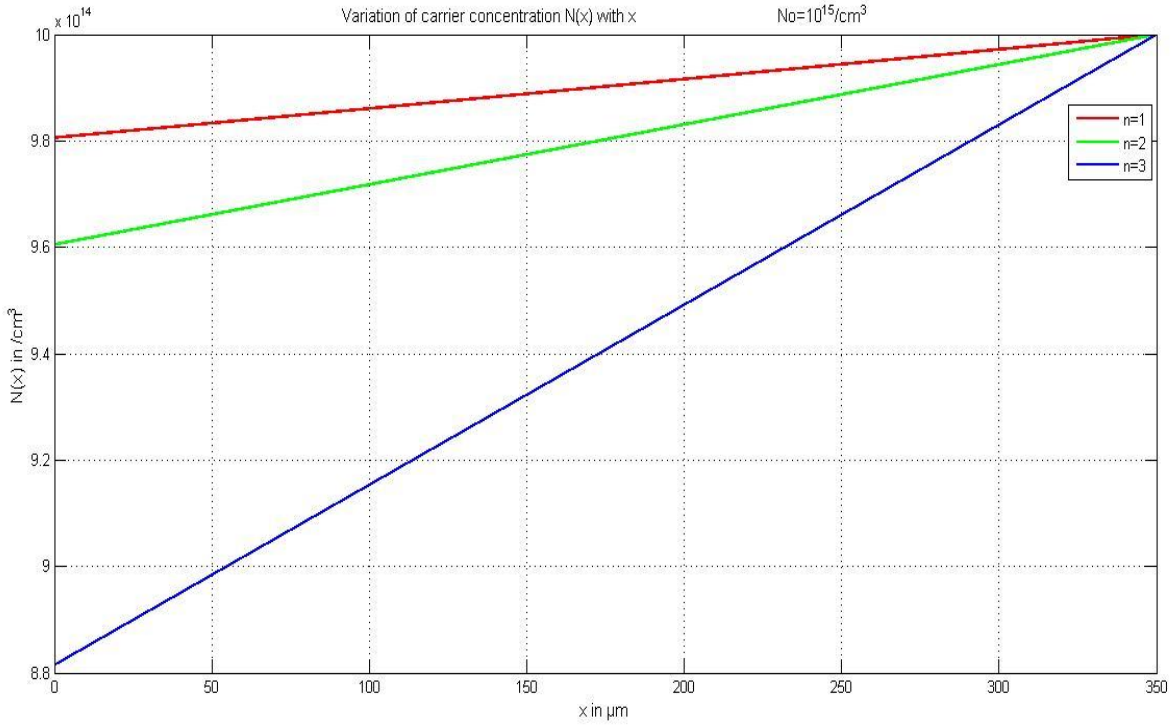

Figure 3.2 Variation of carrier concentration N(x) with x with peak concentration 10^{15} /cm^3.

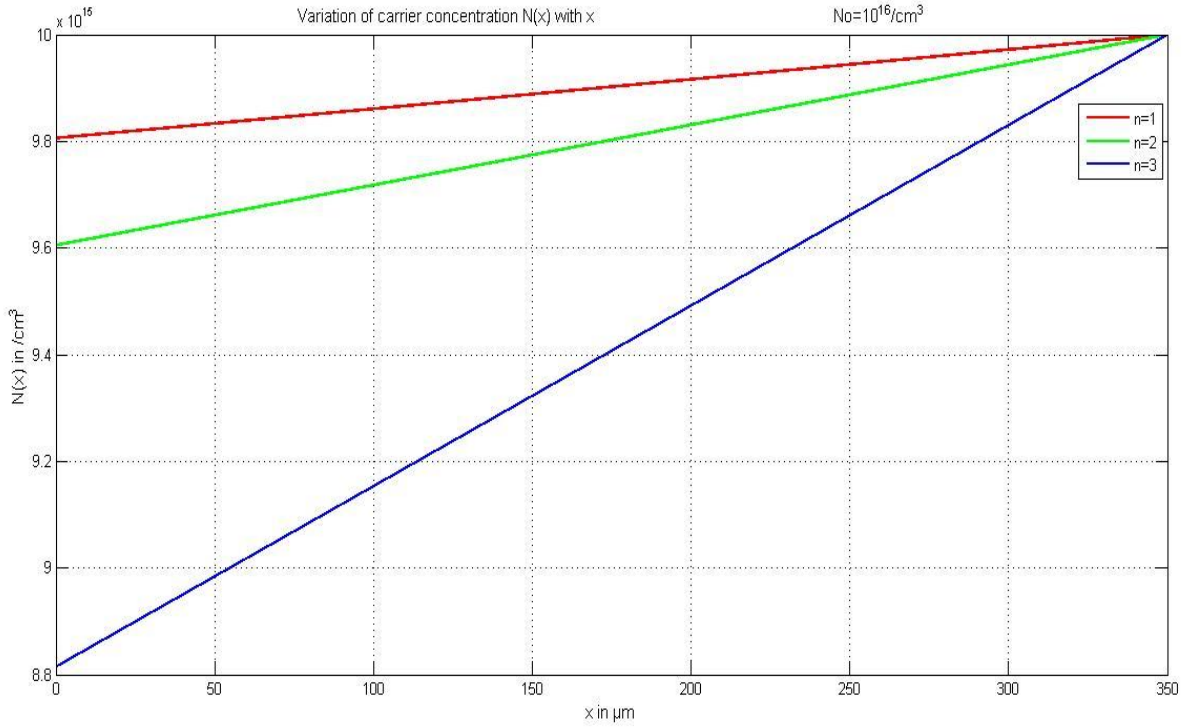

Figure 3.3 Variation of carrier concentration N(x) with x with peak concentration 10^{16} /cm^3.

Figure 3.1 to 3.3 can be combined on a single graph as shown in Figure 3.4. It is seen that increasing peak carrier concentration N_O results in an increase in the carrier concentration gradient α.

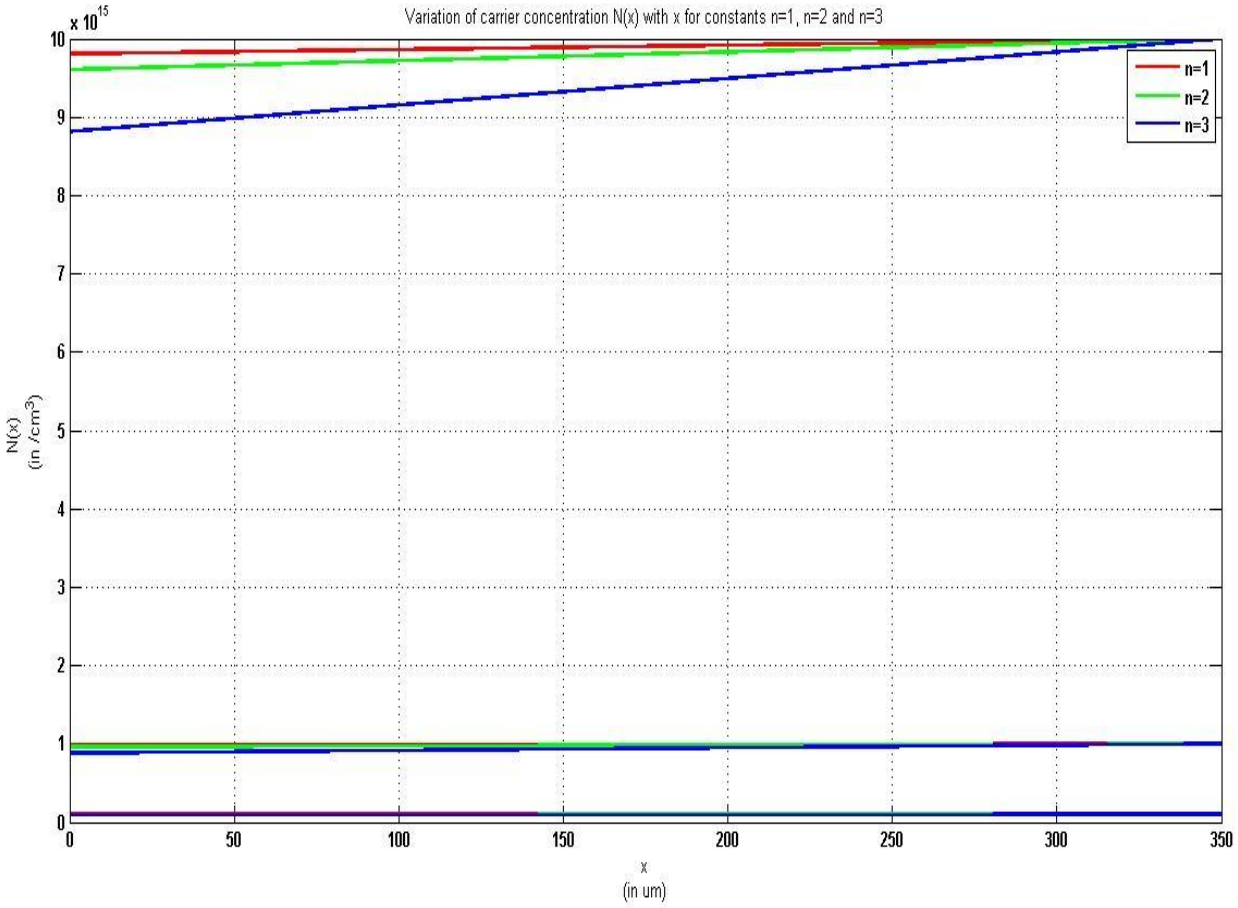

Figure 3.4 Variation of carrier concentration N(x) with x for constants n=1, n=2 and n=3.

Critical electric field (E_c)

For the calculation of critical electric field, complementary error function profile distribution has been approximated as linearly graded profile distribution.

The critical electric field for linearly graded profile is given by the equation,

$$Ec = \left(\frac{e\alpha w^2}{8\varepsilon_s}\right) \quad \text{expressed in V/cm} \qquad (3.14)$$

where

e =electron charge

α = gradient of profile

w =depletion region width

ε_s =permittivity of 3C-SiC semiconductor

Concentration Gradient (α)

The concentration gradient is the slope of the doping profile distribution. It can be calculated by taking the difference of carrier concentration at the base end and at the contact end and then dividing it by the device height.

The concentration gradient is given by the equation,

$$\alpha = \frac{dN}{dx} = \frac{N(x) - N(0)}{x} \qquad \text{expressed in } /cm^4 \qquad (3.15)$$

where

α = gradient of profile

N(x) = doping density at x

N(0) =doping density at the contact

Avalanche breakdown voltage (V_{BAV})

The junction formed by the substrate and drain or source region will conduct a large current if the reverse bias applied to them exceeds a certain value (because the field in the junction near the surface is influenced by the presence of the gate, the above value depends on the gate potential and can be different from

the predicted common pn junction theory). When the device is on, carriers moving fast in the channel can impact on silicon atoms and ionize them, producing electron-hole pairs, this is referred to as impact ionization. The newly generated pairs can gain enough energy to impact on silicon atoms and produce more electron-hole pairs. This is called avalanche effect and is more pronounced in the pinch-off region near the drain where field can be high. Currents larger than those predicted by common device model will then flow, and the phenomenon is referred to as channel breakdown.

For the calculating the avalanche breakdown voltage, complementary error function profile distribution has been approximated as linearly graded profile distribution.

For linearly graded profile the avalanche breakdown voltage is given by,

$$V_{BAV} = \frac{2}{3} E_c w \tag{3.16}$$

Punch through breakdown voltage (V_{BPT})

It occurs in devices with relatively short channels when the drain voltage is increased to the point that the depletion region surrounding the drain region extends through the channel to the source. The drain current then increases rapidly. Normally, punch through does not result in permanent damage to the device [42].

The punch through voltage was calculated using the formula given by,

$$V_{BPT} = \frac{w^3 e\alpha}{12\varepsilon_s} \tag{3.17}$$

CHAPTER 4

Calculation and Results

The present work on 3C-Sic Schottky Barrier diode was undertaken with a view to increasing the magnitude of avalanche breakdown voltage (V_{BAV}) and punch through breakdown voltage (V_{BPT}) beyond 10 kV. The estimated device height has been set at 300 µm but the existing technology for 3C-SiC wafer thickness has been achieved for 200 µm, developed by HOYA Corporation Japan. It is expected that the 3C-SiC wafer thickness can be grown to 300 µm within the next 5years. The profiles used for the wafer doping were three complimentary error functions with function constants n=1, 2 and 3. The peak carrier concentration selected were 10^{14} /cm^3, 10^{15} /cm^3 and 10^{16} /cm^3. These profiles have already been shown in Figure 3.1, Figure 3.2, Figure 3.3 and Figure 3.4. The carrier concentration is a maximum of N_o near base of the device rising to the lowest value over the device height of 300 µm near the contact at the top.

For calculation following parameters have been used:

Permittivity of free space (ε_o) = 8.854×10^{-14} $(\Omega cm)^{-1}$sec
Relative permittivity of 3C-SiC semiconductor (ε_r) = 9.6
Permittivity of 3C-SiC semiconductor (ε_s) = $\varepsilon_o \varepsilon_r$
= 84.9984×10^{-14} $(\Omega cm)^{-1}$sec
Electronic charge (e) = 1.6×10^{-19} C
Peak carrier concentration N_o varied from 10^{14} /cm^3 to 10^{16} /cm^3

All the profiles that have been selected for the study have been shown theoretically to be near approximation to linear graded profile. Hence the gradients as calculated

from equation (3.15) show that for n=1, 2 and 3 the magnitude of gradients of carrier concentration over the device height increases both with the magnitude of carrier concentration and constant n. This is shown in Table 4.1 and Figure 4.1.

Table 4.1 Concentration gradient for different values of N_o and n

Concentration Gradient (α in /cm^4)	$N_o=10^{14}$ /cm^3	$N_o=10^{15}$ /cm^3	$N_o=10^{16}$ /cm^3
n=1	5.515×10^{13}	5.612×10^{14}	5.629×10^{15}
n=2	1.127×10^{14}	1.128×10^{15}	1.128×10^{16}
n=3	3.385×10^{14}	3.385×10^{15}	3.385×10^{16}

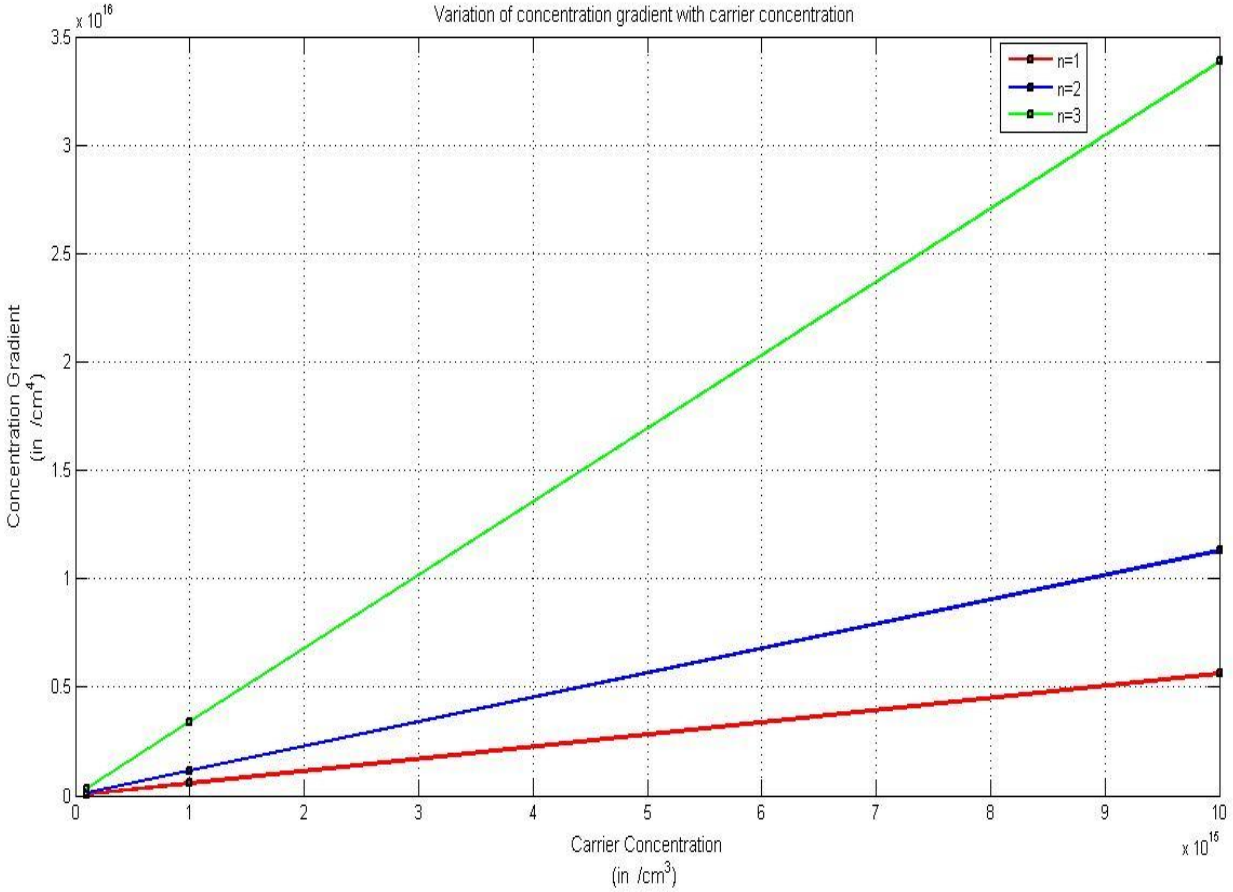

Figure 4.1 Variation of concentration gradient α with peak carrier concentration N_o

The device height as calculated using the equation for linearly graded profile was kept fixed at 300 μm for all profiles. The magnitude of critical electric field E_c ranged from 1.67 kV/cm for $N_o=10^{14}$ /cm^3 and n=1 to 716 kV/cm for $N_o=10^{16}$ /cm^3 and n=3. The avalanche breakdown voltages ranged from 23.38 V to a maximum of 14.3 kV for same values of peak carrier concentration N_o and constant n. These are shown in Table 4.2 and Table 4.3 respectively.

Table 4.2 Critical Electrical Field for different values of N_o and n

Critical Electrical Field (E_c in V/cm)	$N_o=10^{14}$ /cm^3	$N_o=10^{15}$ /cm^3	$N_o=10^{16}$ /cm^3
n=1	1.167×10^3	1.188×10^4	1.19×10^5
n=2	2.38×10^3	2.38×10^4	2.38×10^5
n=3	7.16×10^3	7.16×10^4	7.16×10^5

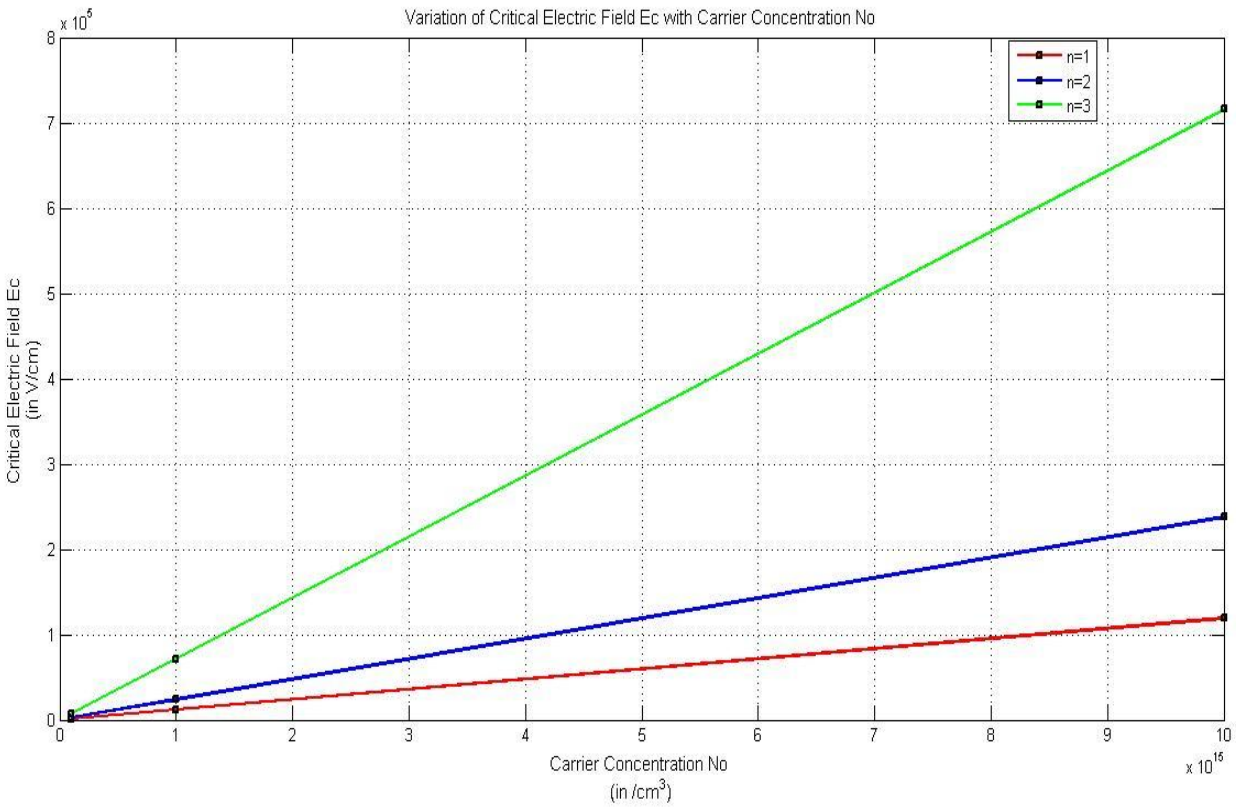

Figure 4.2 Variation of critical electric field E_c with peak carrier concentration N_o

The plot of critical electric field E_c with carrier concentration N_o for different values of constant n is shown in Figure 4.2.

The punch through breakdown voltage and avalanche breakdown voltage which have been found to be equal for all values of N_o and n are plotted in Figure 4.3.

Table 4.3 Avalanche Breakdown Voltage for different values of N_o and n

Avalanche Breakdown Voltage (V_{BAV} in V)	$N_o=10^{14}$ /cm^3	$N_o=10^{15}$ /cm^3	$N_o=10^{16}$ /cm^3
n=1	23.35	237.68	2.38×10^3
n=2	47.73	477.75	4.77×10^3
n=3	143.36	1.43×10^3	14.33×10^3

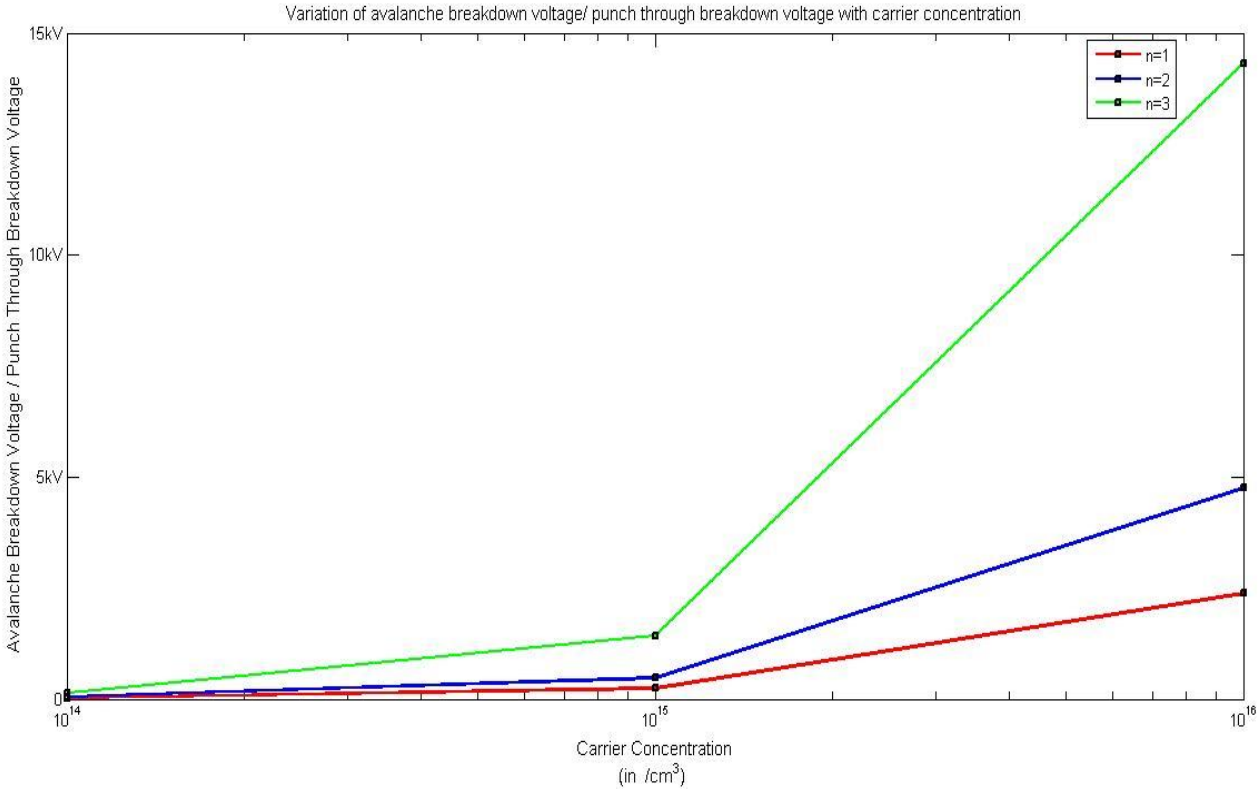

Figure 4.3 Variation of avalanche breakdown voltage/ punch through breakdown voltage with peak carrier concentration

CHAPTER 5

Conclusion and Future Work

Earlier analysis of the complementary error function profiles for carrier concentration in the drift region of Schottky Barrier diodes for n=2 had been quoted in [43]. The present work has been extended to profiles with n=1 and n=3. It is seen that the critical electric field rises linearly with peak carrier concentration N_o for all values of n as shown in Figure 4.2. Our work for n=3 the variation of critical electric field (E_c) is much larger over the same range of N_o than for those with n=1 and n=2.

The avalanche breakdown voltage and punch through breakdown voltage designed here for different values of N_o and n have been found to be equal as shown in Figure 4.3. However there is a drastic rise in the breakdown voltage for n=3 ranging for values of peak carrier concentration from $N_o=10^{15}$ /cm^3 to $N_o=10^{16}$ /cm^3. Hence, it is recommended that the complimentary error function profile with n=3 and $N_o=10^{16}$ /cm^3 should be used for designing 3C-SiC Schottky Barrier diodes with breakdown voltages exceeding 10 kV going up to 14.3 kV.

The analysis quoted here is applicable to devices of 3C-SiC Schottky Barrier diodes with a wafer thickness of 300 µm. Unless and until this wafer thickness is grown in the industry through research and development breakdown voltages of 3C-SiC Schottky Barrier diodes will remain at a much lower voltage than 10 kV corresponding to a wafer thickness of 3C-SiC crystals of 200 µm currently available for device fabrication. The calculated value for 200 µm thick device obtained is about 4.24 kV for peak carrier concentration of $N_o=10^{16}$ /cm^3 and n=3.

REFERENCES

[1] K. Jarrendahl and Robert F. Davis, "Materials Properties and Characterization of SiC, Semiconductors and Semimetals", *SiC Materials and Devices*, vol. 52, pp. 1-20, 1998.

[2] http://che.chonbuk.ac.kr/~nahmks/crystal.htm.

[3] G. R. Fisher and P. Barnes, "Towards a Unified View of Polytypism in Silicon Carbide", *Philosophical Magazine*, vol. 61, pp. 217-236, 1990.

[4] H. Morkoc, S. Strite, G. B. Gao, M. E. Lin, B. Sverdlov, and M. Burns , "Large-Band-Gap SiC, III-V Nitride, and II-VI ZnSe-Based Semiconductor Device Technologies", *Journal of Applied Physics*, vol. 76, pp. 1363-1398, 1994.

[5] O. Kordina, "Growth and Characterisation of Silicon Carbide Power Device Material", PhD thesis, Lonkoping University, 1994.

[6] L. S. Ramsdell, "Studies on Silicon Carbide", *American Mineralogist,* vol. 32, pp. 64-82, 1947.

[7] M. Dudley, W. Huang, W.M. Vetter, P.G. Neudeck, J.A. powell, "Synchrotron White Beam Topography Studies of 2H SiC Crystals", *Materials Science Forum,* vol. 338-342, pp. 465-468, 2000.

[8] H-E. Nilsson and M. Hjelm, "Monte Carlo simulation of electron transport in 2H-SiC using a three valley analytical conduction band model", *Journal of Applied Physics*, vol. 86, pp. 6230-6233, 1999.

[9] W.J. Schaffer, G.H. Negley, K.G. Irvine and J.W. Palmour, "Conductivity Ansisotropy in Epitaxial 6H and 4H SiC", *MRS Proceedings*, vol. 339, pp. 595-600, 1994.

[10] I.A. Khan and J.A. Cooper, "Measurement of High-Field Electron Transport in Silicon Carbide", *IEEE Transactions on Electron Devices*, vol. 47, pp. 269-273, 2000.

[11] H-E. Nilsson, U. Sannemo, and C.S. Petersson , "Monte Carlo simulation of electron transport in 4H–SiC using a two-band model with multiple minima", *Journal of Applied Physics*, vol. 80, pp. 3365-3369, 1999.

[12] H-E. Nilsson, M. Hjelm, C. Frojdh, C. Persson, U. Sannemo and C. S. Petersson, "Full Band Monte Carlo simulation of electron transport in 6H-SiC", *Journal of Applied Physics*, vol. 86, pp. 965-973, 1999.

[13] K. Bertilsson, "Simulation and optimization of SiC Field Effect Transistors", 2004

[14] S. Nishino, H. Suhara, H. Ono and H. Matsunami, "Epitaxial Growth and Electric Characteristics of Cubic SiC on Silicon", *Journal of Applied Physics*, vol. 61, pp. 4889-4893, 1987.

[15] J.W. Palmour, Cree Research, Private Communication, 1996

[16] R.Y. Lakshman, "A Process for Hydrogenation of Silicon Carbide Crystals", MS Thesis, Mississipi State University, USA, 2001.

[17] W.J. Choyke and G. Pensl, "Physical Properties of SiC", *MRS Bulletin*, vol. 22, pp. 25-29, 1997.

[18] P.G. Neudeck, R.S. Okojie, and L-Y Chen, "High-Temperature Electronics—A Role for Wide-Bandgap Semiconductors?" *Proceedings of the IEEE*, vol. 90, pp. 1065-1076, 2002.

[19] R.F. Pierret, "Advanced Semiconductor Fundamentals", Addison-Wesley, Reading, MA, 1987.

[20] S.M. Sze, "Physics of Semiconductor Devices", Willey-Interscience, New York, 1981.

[21] P.L. Dreike, D.M. Fleetwood, D.B. King, D.C. Sprauer, T.E. Zipperian, "An Overview of High Temperature Electronic Device Technologies and Potential Applications", *IEEE Transactions on Components, Packaging and Manufacturing Technology*, vol 17, pp. 594-609 ,1994.

[22] M. Bhatnagar and B.J. Baliga, "Comparison of 6H-SiC, 3C-SiC, and Si for Power Devices", *IEEE Transactions on Electron Devices*, vol 40, pp. 645-655, 1993.

[23] B.J. Baliga, "Power Semiconductor Devices for Variable-Frequency Drives", *Proceedings of the IEEE*, vol. 82, pp. 1112-1122, 1994.

[24] L.M. Tolbert, B. Ozpineci, S.K. Islam and F.Z. Peng, “Impact of SiC Power Electronic Devices for Hybrid Electric Vehicles”, *SAE 2002 Transactions Journal of Passenger Cars - Electronic and Electrical Systems*, pp. 765-771, 2002.

[25] J. Vobecky, “Future Trends in High Power Devices”, *Microelectronics Proceedings (MIEL)*, pp. 67-72, 2010

[26] J. Vobecky, “Design and Technology of High-Power Silicon Devices”, *Mixed Design of Integrated Circuits and Systems (MIXDES)*, pp. 17-22, 2011.

[27] B.J. Baliga, “Power Semiconductor Devices”, Boston, PWS Publishing Company.

[28] T. Ayalew, “SiC Semiconductor Devices Technology, Modeling, and Simulation”, Institute for Microelectronics, Vienna University of Technology, 2004.

[29] B.V. Zeghbroecck, “Principles of Semiconductor Devices”, 2011.

[30] N.F. Mott, “Note on the Contact between a Metal and an Insulator or Semiconductor”, *Mathematical Proceedings of the Cambridge Philosophical Society*”, vol. 34, pp. 568-572, 1938.

[31] J. Bardeen, “On the Nuclear Electric Quadrupole Interaction in Molecular Spectra”, *Physical Review*, vol.72, pp. 717, 1947.

[32] A. Itoh and H. Matsunami, “Analyses of Schottky Barrier Heights of Metal/SiC Contacts and its Possible Application to High-Voltage Rectifying Devices”, *Physica Status Solidi*, vol. 162, pp. 389-408, 1997.

[33] A. Itoh, T. Kimoto amd H. Matsunami, “High Performance of High-Voltage 4H-SiC Schottky Barrier Diodes”, *IEEE Electron Device Letters*, vol. 16, pp. 280-282, 1995.

[34] A. Itoh, T. Kimoto amd H. Matsunami, “Excellent Reverse Blocking Characteristics of High-Voltage 4-SiC Schottky Rectifiers with Boron-Implanted Edge Termination”, *IEEE Electron Device Letters*, vol. 17, pp. 139-141, 1996.

[35] D. Alok and B.J. Baliga, "SiC Device Edge Termination using Finite Area Argon Implementation", *IEEE Transactions on Electron Devices*, vol 44, pp. 1013-1017, 1997.

[36] M. Roschke and F. Schwierz, "Electron Mobility Models for 4H, 6H, and 3C SiC[MESFETs]", *IEEE Transactions on Electron Devices*, vol 48, pp. 1442-1447, 2001.

[37] M. Sochacki, J. Szmidt, A. Werbowy, and M. Bakowski, "Current-Voltage Charateristics of 4H-SiC Diodes with Ni Contacts", *Journal of Wide Bandgap Materials*, vol. 9, pp. 307, 2002.

[38] X. Jorda, D. Tournier, M. Vellvehi, A. Perez, R. Perez, P. Godignon, J. Millan, "Comparitive Evaluation of High Current SiC Schottky Diodes and Si PN Junction Diodes", *Spanish Conference on Electron Devices*, pp. 87-90, 2005.

[39] J.W. Palmour, "Energy Efficient Wide Bandgap Devices", *Compound Semiconductor IC Symposium*, pp. 4-7, 2006.

[40] R. Talwar and A.K. Chatterjee, "A Method to Calculate the Voltage-Current Characteristics of 4H SiC Schottky Barrier Diode", *Maejo International Journal of Science and Technology*, vol. 3, pp. 287-294, 2009.

[41] R.J. Michael et.al., "Innovative 3C-SiC on SiC via Direct Wafer Bonding", *Materials Science Forum*, vol. 740-742, pp. 271-274, 2013.

[42] A.D. Sedra and K.C. Smith, "Microelectronis Circuits," Oxford University Press Inc., New York, 2004

[43] Chandrakant Verma, "An Analytical Study of 6H-SiC Schottky Barrier Diode (SBD) using Complementary Error Function Profile for Breakdown Voltages and Depletion Region Width", M.E. Thesis, 2009.